Novel embryonic stem cell-infused scaffold for peripheral neuropathy repair

A Thesis
Presented to
The Academic Faculty

by

Justin Ryan Papreck

In Partial Fulfillment
of the Requirements for the Degree
Master in the
School of Biomedical Engineering

Georgia Institute of Technology
August, 2008

Novel embryonic stem cell-infused scaffold for peripheral neuropathy repair

Approved by:

Dr. Yadong Wang, Advisor/
School of Biomedical Engineering
Georgia Institute of Technology

Dr. Ravi Bellamkonda
School of Biomedical Engineering
Georgia Institute of Technology

Dr. Phil Santangelo
School of Biomedical Engineering
Georgia Institute of Technology

Date Approved: 04/14/08

Table of Contents

List of Figures

List of Symbols and Abbreviations

PGS	poly [glycerol sebacate]
Epo	Erythropoietin
EpoR	Erythropoietin Receptor
NGF	Neural Growth Factor
BDNF	Brain-Derived Neurotrophic Factor
GDNF	Glial-Derived Neurotrophic Factor
TNF α	Tissue Necrosis Factor-α
IL-1β	Interleukin-1β
ROS	Reactive Oxygen Species
SOD	Superoxide Dismutase
Gpx1	Glutathione Peroxidase
Sod1	(cytosolic) Cu, Zn-SOD
Sod2	(mitochondrial) Mn-SOD
NGC	Nerve Guidance Channel
FGF	Fibroblast Growth Factor
ES	Embryonic Stem Cell
hES	Human Embryonic Stem Cell
TCPS	Tissue Culture Polystyrene
IP	Intraperitoneal (injection)
CNS	Central Nervous System
SFI	Sciatic Functional Index

Summary

Peripheral nerve injury in adults often leads to permanent functional loss with or without pain. Traumatic injury or surgery, metabolic injury (diabetic neuropathy), and drug toxicity can lead to neuropathies and all negatively impact the quality of life[1-8]. Damage to the nervous system is often permanent since neurons in the brain and periphery are post-mitotic and have limited regenerative capacity. Nerve repair involves axon regeneration, a complex and incompletely understood process with repair potential declining with age[9-15].

The research and design discussed involves the induction of endogenous repair mechanisms of the peripheral nerve using embryonic stem cells, alginate hydrogel, and the guided support of a biomaterial scaffold composed of PGS. Three different populations of cells are discussed: human embryonic stem cells, neural progenitor cells derived from human embryonic stem cells[16], and primary rat bone marrow stromal cells. This study was innovative in that it was the first attempt for use of an elastomeric biomaterial scaffold in an *injury model* for the purpose of *clinical application*. This research is significant as it has direct *clinical relevance* in that it incorporates both *functional and neuropathic recovery* of patients affected by peripheral nerve damage.

Chapter 1

Introduction

Physiology of Peripheral Nerve Trauma

The physiological response to a peripheral nerve injury is the sprouting of neurites from the proximal stump of the damaged nerve, while the distal nerve undergoes Wallerian degeneration, a programmed process that involves the degradation of the myelin sheath, segmentation of the axon, 'dedifferentiation' of Schwann cells to non-myelinating cells, and infiltration of macrophages[17-21]. Specifically this change occurs via an influx of calcium ions through specific channels that activate proteases which subsequently degrade the axolemma and axoplasm of the distal nerve[19, 22-24]. Although the regenerating proximal axon must cross to the injured or severed distal nerve, there is no reconnection of the tissues, but rather new growth through an optimized track for reinnervation of the distal tissue[25, 26]. In cases where the axon and dendrites sprout laterally innervating new tissues, the result is an increase of neuropathic pain thus it is crucial to promote nerve guidance in the correct path as soon as possible[17, 18, 24, 25, 27]. During this axonal migration, the Schwann cells begin to dedifferentiate, also taking on a different phenotype and role incompletely understood[17, 18, 24].

One of the changes in the Schwann cells during this process is the upregulation of Epo and Epo receptors on their surface, providing a target for Epo signaling which may play a role in subsequent nerve regeneration[21]. Epo is a hematopoietic cytokine that has been shown to be neuroprotective in ischemia[28] and after crush injuries[29], possibly acting as an antagonist to inflammatory cytokines[30]. Epo binds to EpoR which triggers dimerization and stimulation of Jak2, a Janus kinase, which in turn activates extracellular signal-regulated kinase (ERK/MAP), which is responsible for cell proliferation[21]. The relationship between

the hypoxic upregulation of Epo and cell proliferation lies in that proliferated erythrocytes can systemically deliver more oxygen reaching the hypoxic site, thus downregulating Epo.

Epo is known to promote the neurotrophic effects of proliferation and differentiation[31] as well as reduce neuropathic pain resulting from nerve injury[29, 32]. As the Schwann cells dedifferentiate, no longer attached to the axon, they begin to proliferate and form the Bands of Büngner, which provide support and guidance from the proximal nerve stump to the distal stump[19, 20]. Another change that the Schwann cells exhibit is the down-regulation of myelin-associated genes, and up-regulation of neurotrophic factors including NGF, BDNF, and GDNF as well as interleukin-6 and leukemia inhibitory factor which are both cytokines[20]. Despite the upregulation of trophic factors and other means by which the nerve can self-repair, many cases are too severe for endogenous repair ultimately resulting in a loss of function as well as the addition of neuropathic pain. Other causes of neuropathic pain are a result of misdirected axonal sprouting, organizational changes in central nuclei, and hyperinnervation; all phenomena associated with 'successful' regeneration[25, 26, 33, 34].

Characteristics of Neuropathic Pain

Neuropathic pain is pain resulting from insult to the peripheral or central nervous system[35] and affects approximately 1.8 million people in the United States[36]. Neuropathic pain (as opposed to nociceptive pain) has a particular pattern including extreme reaction to non-noxious stimuli (allodynia) and hyperalgesia. The aforementioned causes of peripheral nerve damage: physical trauma, metabolic injury, and drug toxicity all follow as causes for neuropathies[1-8]; however the mechanisms for neuropathic pain are incompletely understood. The physiological response to intense or damaging noxious stimuli is the triggering of high-threshold nociceptor primary sensory neurons, eliciting a painful response[37]. This is

different from spontaneous pain, or pain elicited from non-noxious stimuli without triggering the sensory neurons, characteristics of neuropathic pain – pathological pain.

Several tests have been established to provide quantitative measures with neuropathic pain, focusing on the allodynic and hyperalgesic effects of the neuropathies. One model that has aided this study significantly is the chronic constriction injury model (CCI) introduced by Bennett and Xie[38]. This model uses 4 sutures to constrict the sciatic nerve, which ultimately induces pain consistent with human patients exhibiting neuropathic pain. Quantitative measures have been applied to mechanical allodynia using Von Frey filaments, weighted filaments dropped on the paws of the test subjects, and hyperalgesia using hot and cold plates measuring the latency of paw withdrawal.

Treatment of neuropathic pain is often limited and unsuccessful. Patients with neuropathic pain are typically insensitive to opioids and other non-steroidal anti-inflammatory drugs[37]. This pain is typically treated pharmacologically with tricyclic antidepressants, serotonin and norepinephrine uptake inhibitors, and anti-epileptics; however there is limited efficacy and often undesirable side-effects with such treatments[37, 39, 40]. Recent studies have also shown that exogenous Epo can be used to reduce neuropathic pain by regulating pain producing cytokines[29].

The response to pain is in conjunction with an inflammatory response introducing bradykinins, TNFα, endothelins, hydrogen ions, substance P, IL-1β, NGF, prostaglandins, histamine, and ATP, as well as an accumulation of sodium channels increasing the number of spontaneous ectopic discharges[29, 39-41]. Endothelin-1 is suspect to cause neuropathic pain as well as TNF-α[41-43]. One type of Endothelin receptor, ET_A, has been shown to participate in the inflammatory reaction, triggering an algesic pathway. Contrarily, ET_B shows the opposite effect, triggering an endogenous analgesic pathway that ultimately up-regulates

opioid receptors on nociceptors[42, 44]. Another suspect to neuropathic pain is the inappropriate reinnervation following nerve injury; the sprouting of new nerves with new undirected targets[26].

Because of the poor understanding of neuropathic pain, there are very few treatments for it, and those which are available have relatively low efficacy. Neuropathic pain is one inherent problem with neural damage, and despite its poor understanding, it is critical to regulate and reduce in the clinical setting. Due to the nature of neuropathic pain and the pathologies it is associated with, neuropathies and neuropathic pain increases with the age of the patient. Aging not only affects the pain, however, it also affects the overall regenerative response on both the gross level as well as the cellular level.

Aging and Nerve Regeneration

Age-specific morbidity rates for pain increase per decade of life, with a prevalence as high as 67-80% among the elderly[45-47]. Prevalence of neuropathic pain follows this trend, also increasing with advancement in age, with decreasing potential for full recovery[10-13, 15]. One factor that induces nerve damage with elevated effects in age is insult from reactive oxygen species, which play a role in abnormalities in nociceptive processing[48, 49]. There is an excess of generated ROS in peripheral nerve injuries, and to further exacerbate this problem, the enzymatic activity and mRNA expression of the antioxidant SOD and catalase decrease as a function of age[48, 50, 51]. Despite the increase in occurrence across age groups, the magnitude of neuropathic pain symptoms is not significantly different; however the rate of recovery is significantly reduced in older subjects[52, 53]. The age-related decrements in endogenous antioxidant defense severely predispose cells for free-radical damage, thus creating an increasing potential for neuropathies with age[53].

In the cell, there are three primary mechanisms by which the oxidative stress is ameliorated. Catalase, found in the peroxisomes, superoxide dismutatases found in the cytosol and mitochondria, and GPx1 found throughout the cell. There are two predominant types of SOD in humans, Sod1 and Sod2, the cytosolic and mitochondrial SODs respectively. The SODs both catalyze the reaction changing intracellular superoxide ions into oxygen and peroxide, while catalase and GPx1 both breakdown the peroxide molecule into water. With compromised machinery in these enzymes, there is great potential for oxidative damage by the accumulating superoxides and free oxygen radicals. This is linked to aging by the aforementioned decreases in mRNA expression with age, thus demonstrating the criticality of irreparable cells depending on these mechanisms for lifelong survival.

Current Therapies for Peripheral Nerve Damage

The current therapies for peripheral nerve repair are limited; the most successful procedure in nerve repair is autologous nerve grafting which requires removal of a healthy nerve from elsewhere in the body and generally provides incomplete recovery. Short gap nerve transection does not require the graft of additional nerve tissue; however, one shortcoming in both procedures is damage from sutures as well as incomplete recovery of the distal nerve. Some advances have been made improving upon this procedure including the use of fibrin glue in lieu of nylon sutures[26, 54-59]. Despite the success of fibrin as a suture material, the efficacy of the graft itself is limited.

Many engineering approaches to address the limited efficacy of the autograft have provided new means for peripheral nerve repair. Biomaterials have been used to directly affect the nerve regeneration or as a scaffold to support cells which affect regeneration. The most promising results have come from the NGC, a biomaterial tube through which each

end of the lesioned nerve is inserted, encouraging/directing the nerves to path-find and fuse to its severed distal stump. Different cell populations have also been used to implant with the scaffolds, but Schwann cells have been the primary focus as they are known to play a critical role in peripheral nerve regeneration. Despite the many materials, cells, and modifications to these engineered approaches, none have significantly improved upon autologous grafting.

NGCs have been constructed from many different biomaterials, each with different physical and chemical characteristics. Some of the most common materials used to construct NGCs have been poly[lactic-co-glycolic] acid[60-64], poly[L-lactide-co-6-caprolactone][65-67], poly[phosphoester][68, 69], poly[L-lactic] acid[61, 70, 71], gelatin[72-74], chitosan[75-82], and several hydrogels (as nerve guidance *materials* rather than channels)[83-98]. Aside from using different materials, some studies focused on the modification of existing material channels/scaffolds using growth factors (NGF, BDNF, FGF, GDNF)[69, 71, 99, 100], surface modification (smooth vs. rough/micropatterned)[69, 78, 83, 101-103], and implantation of Schwann cells[62, 77, 87, 89, 94, 103-112]. As previously mentioned, despite these many modifications and promising enhancements, none of the engineered implants have significantly improved upon autologous nerve grafting[60, 62, 68, 82, 83, 101, 102, 113].

Failures of these attempts at improved nerve regeneration may be a result of a culmination of factors including undesirable immune response, inability of neurotrophic factors released from the proximal stump to reach the distal stump, lack of a defined matrix to support the regenerating nerve, inappropriate material characteristics, and in some cases the lack of Schwann cells in the immediate area[64, 114, 115]. Geometry, porosity, biodegradability, biocompatibility, polymer chemistry, mechanical strength, and elasticity all affect the ability for axon growth *in vivo*[116-118]. The balance of the scaffold properties, support

cells, growth factors, and the extracellular matrix ultimately regulate the neuro-regenerative potential with hopes to optimize neural potential by inducing conditions mimicking the embryonic stage of nerve growth[61].

The scaffold provides the structure for the support cells as well as the nerve throughout regeneration, but predominantly during the initial phase, thus it is important that the material have an appropriate degradation rate, porosity to allow for cell recruitment as well as nutrient and gaseous exchange, mechanical strength to support the tissue, and elasticity similar to that of the tissue so as not to impede growth of the axon. PGS is a unique material in that it is biocompatible, maintains its structural integrity throughout its biodegradation, and has elastomeric properties similar to that of nerve tissue[116-120]. PGS implants gradually lost mechanical strength, about 8% per week, characteristic of surface erosion[117]. The implants maintained geometry after implantation up to 35 days, and completely absorbed within 60 days[117]. Additionally, the elastomeric property of PGS makes it ideal for work with nerve tissue, having a Young's modulus of 0.5MPa[117] compared to that of nerves: 0.45MPa[119]. PGS scaffolds have also been shown to support several different cell types *in vitro* as well as Schwann cells *in vivo*[78, 116-118].

Although PGS use alone seems ideal for implantation, the density at which stem cells are seeded at has been shown to influence the cell fate *in vivo*[121]. Similarly, the distribution within a hydrogel bead has been demonstrated to alter the capability for cells to migrate due to the ability to form a matrix network[122]. These parameters cannot be controlled using the solid PGS scaffold alone, thus an alginate hydrogel will be employed to specifically control the cell density, distribution, and gel density to allow for migration. These may prove to be crucial in limiting teratoma formation as well as allow for proper intercellular chemotransduction.

Use of Stem Cells in Nerve Regeneration

Schwann cells have been the focus of support cells for many groups working with NGCs with limited success[62, 77, 80, 83, 102, 103, 105, 106, 109, 111, 115, 123-125]. Adjuncts to the NGC have included stem cells in lieu of Schwann cells; particularly stem cells which have the potential to differentiate into both neural and support cells. Human embryonic stem cells are one type of stem cells that are currently being used in these studies[126-128]. hES cells are a pluripotent population of cells derived from the human embryo, capable of differentiating into the three separate germ layers, and have been demonstrated to differentiate into neuronal tissue *in vitro*[129-132]. The aforementioned neural progenitor cells are derived from hES cells through a specific protocol. Benefits in using NPCs rather than hES cells include problems with teratoma formation that is common with ES cells[133-135]. However, the pluripotent nature of ES cells provides an opportunity for differentiation into the support cells needed for neural regeneration, as well as possibly providing an "embryonic phenotype" in the damaged region, creating the necessary environment for optimized axonal growth[136]. Recent advances in understanding ES cell motor differentiation[16, 43, 137-142] underscore the potential of these cells for therapeutic peripheral nerve regeneration, especially if the cells can be implanted on an optimal scaffold or hydrogel[90, 125, 143-146].

Chapter 2

Development of a Working Scaffold

This chapter discusses the methods and approaches taken in the development of a PGS scaffold that maintains mechanical integrity and supports cell growth and maintenance. In order to optimize the scaffolds for further use *in vivo*, a thorough *in vitro* study of the behavior of cells on the biomaterial scaffold was essential.

The design of the initial scaffold used a microfabricated silicon mold as the template, while later designs used the principle of salt fusion to provide the scaffolds. While the target for each of the technologies was slightly different, both did show potential for any future studies with this material.

Using Microfabrication to Make a Delivery Network

The design to be implemented was based on capillary branching patterns to ensure the appropriate diameter and bifurcation angle for physiological fluid properties. In order to do this, the design was put in two dimensions using AutoCAD2005 software which was then sent in to a company who provided us with a glass mask with the negative of the design. A coat of photoresist polymer was evenly spun onto the silicon plate to which the mask was to be transferred, and then exposed to UV light for the calculated time for the thickness of photoresist.

Because the mask that was ordered was glass, rather than quartz, UV rays did not pass through, and the photoresist did not maintain the desirable pattern. Furthermore, the machinery needed in the clean room to perform Bosch etching was the most sought after

machinery, making it very difficult to get training on. With expenses related to keeping students in the clean room as well as the difficulty in getting training and improper mask, this technique was abandoned. Furthermore, previous studies with this technique had demonstrated an uneven distribution of cells, with clusters only in the bifurcations[120].

Observing the Migratory Response of Cells

One of the major premises behind this design was the ability for cells to migrate through the major clusters to fill in the gaps. While microfabrication was abandoned, a series of simple "wound assays" (also known as scratch assays) were performed on PGS, glass, polystyrene, as well as laminin-coated PGS, glass, and polystyrene. Furthermore, one set of each of these was left in ambient air conditions (20% oxygen) while the other group was maintained in 6% oxygen.

Using a sterile 200μL pipetter tip, a scratch was made across each of the substrates. For the next 36 hours, each plate was photographed under the microscope once every 3 hours to monitor the acceleration and rate of the migration. We had hypothesized that the normoxic (6% O_2) cells would migrate more rapidly than the ambient cells.

Unfortunately, because of the exposure to ambient air pressure during the photography of the plates as well as inconsistencies in heat throughout the experiment, the many degrees at which the two sets varied continued to increase toward the end of the experiment, and furthermore, many of the plates started observing lifting of the cells, and rapid cell death from the movement of the fluid back and forth to the incubator to the extent that there were not enough plates in any set to gather any statistically conclusive evidence for anything.

We discussed an automated design for both this and the aforementioned design, however, with the many setbacks these ideas were set aside and a new design was brought forth.

Salt Fusion-Based Scaffolds for Nerve Regeneration

This was a design based on an old technique in biomaterials, utilizing different solubilities of the biomaterial and salt[147]. A salt, in our case Sodium chloride, fills a mold and is subjected to high humidity for a given amount of time allowing it to fuse together forming a complete negative mold for the polymer. The polymer is poured over the dry salt structure and cured. Once cured, water is used to dissolve the salt matrix, while the material remains in-tact.

The initial molds were a very simple design milling a trench in a strip of solid PTFE. The 12mm trench was designed to be both 5/32" wide and deep with an open surface for the salt to be poured in. A second cut was made to fit a 1/16" PTFE coated needle to function as a lumen. These dimensions were chosen as they are the size of the sciatic nerve in rat (1/16"), and a substantial but not intrusive thickness for cell seeding and maintenance.

Up to seven of these trenches were made on a single block of PTFE. After several cures, the PTFE started to warp causing a variation in the size of each scaffold depending on their position. To rectify this problem I attempted to remove the salt scaffolds before curing the PGS at the higher temperature, but to no avail. Another problem encountered was non-uniform curing of the scaffolds. The first attempt to fix these problems was to create the molds in aluminum however I wasn't able to machine the aluminum such that it would release the scaffolds even when coated with a lecithin release spray.

To overcome these problems as well as to get a fully circular shape, I designed the molds to have an upper and lower half which would be taken apart after the fusion of the salt. Following removal of the salt, the polymer would be applied to the salt templates on a flat piece of PTFE. These would be cured suspended above the surface, also providing a more uniform curing. In essence, this was the most effective method I attempted, however I was getting anywhere between a 25% and 75% yield at the end of the process.

Scaffold Fabrication

Poly (glycerol sebacate) (PGS) is synthesized as previously reported[117]. Porous PGS scaffolds are prepared using a salt fusion method[147] modified to accommodate the properties of PGS. We used 1/16" polytetrafluoroethylene (PTFE) tubing covering 20 g needles (rat sciatic nerve is about 1mm in diameter[66] ~ 19 g) embedded 1mm in the salt in a PTFE mold. The mold is incubated at 37ºC and 88% relative humidity for 150 minutes and then dried in a vacuum oven at M60ºC and 100mTorr overnight. PGS dissolved in tetrahydrofuran (THF) is repeatedly added to the salt mold and allowed evaporate in a fume hood for 60 minutes. The mold is then cured in a vacuum oven at 150ºC and 100mTorr for 24 h. After cooling, the PGS/salt molds are soaked in dH_2O for 24 hours, exchanging the water every 4 hours for the first 12 hours. Scaffolds are then lyophilized and stored dry until use. A series of ethanol washes is performed to remove any excess monomer prior to conditioning in medium. While the inner diameter of the scaffolds is 18 g, the outer dimensions of the scaffolds will be varied to compensate for degradation and surface area for cell adhesion.

Making the Scaffold Work In vitro

While still working on making the scaffolds, the first set of *In vitro* experiments involved N27 mouse neural progenitor cells plated on flat PGS, glass, and TCPS in at 20% oxygen

[Figure 1]. Although it was hypothesized that the N27 cells would proliferate over time, the contrary was found. Because N27 cells had no impact on the future cells to be used in the study, these were no longer used, but instead primary bone marrow cells extracted from the femurs of rats. Similarly because the nature of the 2D plate and 3D scaffold is so different, the cells were directly applied to scaffolds following removal and observed after 3 different time points **[Figure 2]**. Some problems with this second assay were that I was still using the initial scaffold design, so there was not uniformity in size or cross-linking density amongst the scaffolds. Also, in calculating the values from the standard curve, when applied to the actual data obtained, the values for the latter two data were negative. When repeated, the same results were obtained.

The next assay examined the difference between different surface modifications as well as different oxygen conditions. Fibronectin and laminin were adsorbed to uniformly produced PGS scaffolds. Scaffolds with the adsorbed proteins as well as without were seeded with primary bone marrow stromal cells obtained from rat. Half of the scaffolds were placed in 6% oxygen while the rest were left in ambient conditions and cultured for 7 days **[Figure 3]**. The results indicated that the laminin-coated scaffolds were not different from the null either oxygen condition, however, fibronectin was significantly higher than the null, but only in 6% oxygen. With a similar trend, the control scaffold of unmodified PGS also had a significant difference between the 6% and 20% oxygen supporting the hypothesis that culture would be better supported at conditions representative of the *in vivo* environment.

Discussion

The initial focus of this project was the implementation of a technology integrating cells and cell behavior with the biomaterial poly (glycerol sebacate). The initial design utilized microfabrication to create a micro-array of capillaries through which a 3D network could be established. The theory behind this technology is still sound, however the cost and resources available were limited at the time, and this was discontinued. Furthermore, the previous attempts at gaining confluence throughout the network had not been successful. With the initial momentum of the project being migration of cells, the full design would have encompassed a full closed system to observe the behavior of the cells 24 hours a day while being fully automated to track different positions on a plate.

Keeping cell migration as the main task, the secondary steps involved simple wound assays which were assayed with different ligands as well as under different oxygen tensions. While working in low oxygen, I discovered it was nearly impossible to keep the plates from repeated spikes of exposure to 20% oxygen while taking photographs of them. And due to the rate at which cells normally migrate, which is on the order of 24-36 hours, the only way that could circumvent these problems would be to either take pictures in a 6% oxygen chamber or to utilize a closed system that could maintain the low oxygen over the time period necessary. This however, was not done as the total focus of the research was changed to something that could more readily use PGS.

The making of PGS scaffolds used a very simple process with several conditions that were easily controlled, however this proved not to be so simple in the producing of uniformly sized and cross-linked scaffolds. The technologies that had been used in the lab prior to my experiments worked on a much larger scale, typically at least ten times larger. Many of the problems faced in this research with the initial design were due to fluidics,

balancing the viscosity of the material with the capillary action of the salt scaffold, and even gravity. Other problems arose because when a small break occurred on the larger scale, say a 1mm break, they lost at best 1% of their scaffold, where a 1mm break cost the smaller scaffold 10%, and thus could no longer be used. This was a problem with all designs, as when lifting the scaffold out of the PTFE mold was the first point of potential breakage as there was a vertical force applied by the thin needle in the lumen to the thin cylinder. The second potential breaking point was in the removal of the needle, as the scaffold was placed back in the mold while the needle was removed axially. The third breakage could occur when removing the 'free' salt scaffold from the mold again…often times the light tapping would cause breaks or the scaffold would break as it fell 10mm.

Because of all of these potential breaks in the scaffold prior to even adding PGS, there was a low yield. On top of these problems, there was still no insurance that 100% of the samples were even going to be uniformly filled, as the PTFE is opaque and must be filled across both sides evenly. Using a number of these molds with the exact amount of salt needed, I was eventually able to reach a yield of 75%.

Following the fabrication, the *in vitro* studies were designed to show the viability of the scaffolds with cells prior to the *in vivo* studies. During the initial *in vitro* assay in which N27 cells were grown on PGS-coated plates, the data shows a decline over time rather than proliferation **[Figure 1]**. This indicated that the PGS plate was toxic to the N27 cells. This was attributed to monomers attached to the surface of the PGS which would be more thoroughly removed in future studies.

Instead of continuing with N27 cells, the experiment shifted to the use of primary bone marrow stromal cells extracted from rat femurs, isolated and then immediately put into the scaffolds for culture. As seen in **[Figure 2]**, there is a similar decline over time, however not

as extreme as seen with the N27 cells. This assay was expanded to observe differences with oxygen tensions and ligands bound to the surface of the scaffold. After 7 days in culture, the number of cells is extremely low compared to the number of cells that were seeded. Similarly the only samples that were significantly different in fluorescence from the null were the control and the fibronectin-coated. While this assay did show there was a significant difference between 6% and 20% oxygen by ANOVA analysis, the low quantity of cells remained a problem for this experiment in general. Despite these resulting low cell numbers on PGS scaffolds, there has been evidence that demonstrates that other cell types: Schwann cells[116], fibroblasts[117, 118], and even non-robust cardiomyocytes thrive on PGS scaffolds[148, 149]. These contrasting results demonstrate that it is not the properties of the PGS causing the cell death, but rather an interaction between the particular cells worked with in my experiments with the PGS.

The next step in the design was going to use alginate to encapsulate the cells and hold them within the scaffolds. The final step in this project was the demonstration that alginate can be used to encapsulate and permeate the PGS scaffold.

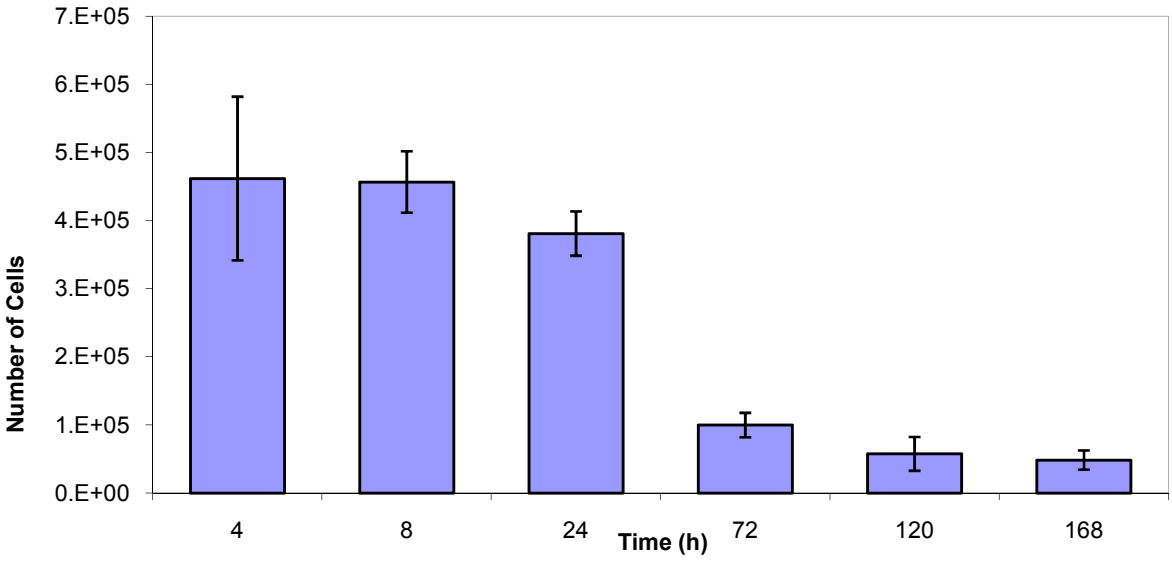

Figure 1: Number of N27 cells grown on a flat plate of PGS as an expression of time.

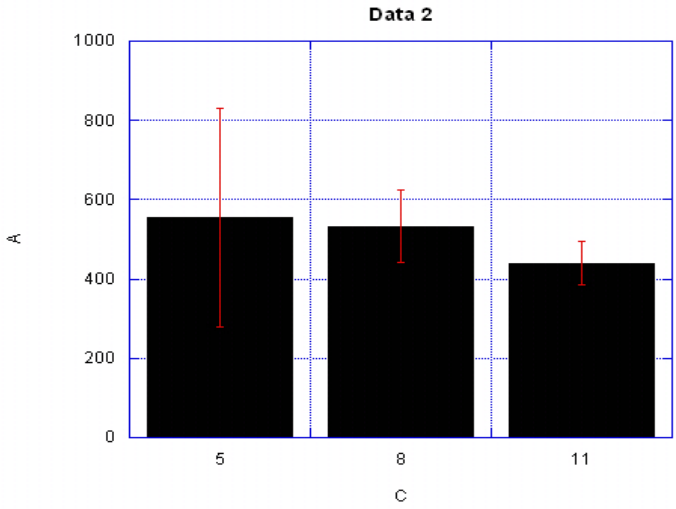

Figure 2: Arbitrary units of fluorescence representing marrow stromal cells cultured in PGS scaffolds over 5, 8, and 11 days. Note: units are arbitrary because in calculating the standard curve, days 8 and 11 would be negative numbers.

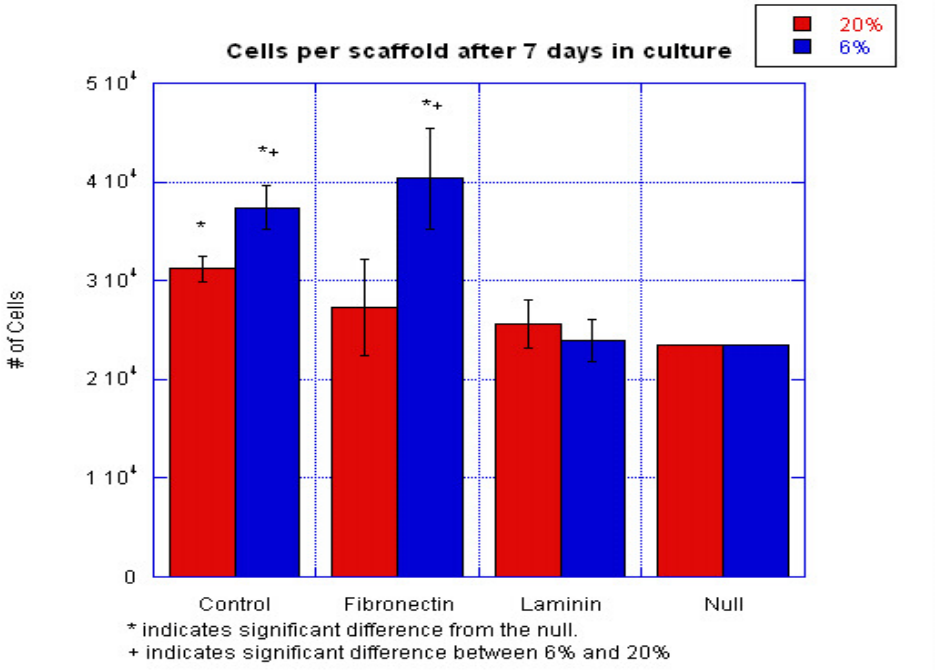

Figure 3: Cells per scaffold after 7 days of culture. Null represents no cells grown on scaffold. Control represents no modification of scaffold.

Chapter 3

Experimental Methods for Potential Study

This chapter discusses the experimental design following the procedures establishing a basis for future studies. While these experiments were not fully or at all performed, a fully detailed experimental design was established after months of literature research and careful planning. If this research is to be continued, this is the proposed design.

Conditioning and Training Rats for Behavioral Testing

In order to perform any form of behavioral analysis, a baseline must be obtained. And in order to gain a regular baseline, the rats must be handled and accustomed to the setting where the experiments will be performed for several weeks prior to the experimentation. The tests the rats were being prepared for including controlled external stimuli applied to the paws of the rats, thus the rats are placed in a specialized cage in which stimuli could be applied from above and below.

In addition to the cage, the rats are also conditioned to walk freely on a large piece of white paper, and after initial conditioning, they have their paws dipped in ink to quantify their gait. Ultimately, there are two general tests to be performed pre and post-surgery with the rats: motor function assessment and functional recovery behavioral evaluation.

Motor function will be assessed by a basic motility test, the sciatic functional index (SFI)[150, 151]. These indices are obtained by wetting the hind feet with 20% methyl blue and allowing them to walk freely in a paper-lined corridor and comparing the experimental footprint to the normal. Paw print length (PL), distance to opposite foot (TOF), total toe

spreading (TS), and intermediate toe spreading (IT) are measured to determine the SFI **[Figure 4]**. Rats will be analyzed for pain and functional recovery up to 60 days. The sciatic functional index is determined by the following equation (where E and N are experimental and normal respectively)[152]:

$$SFI = \frac{ETOF - NTOF}{NTOF} + \frac{NPL - EPL}{EPL} + \frac{ETS - NTS}{NTS} + \frac{EIT - NIT}{NIT} X \frac{220}{4}$$

Pain after injury will be assessed by quantitating thermal and mechanical hyperalgesia. Baseline paw withdrawal latency (PWL) to thermal stimulus will be used to assess the thermal sensitivity. A radiant heat source directs a thermal stimulus to the paw, and a photoelectric cell detects light reflected off the paw so that when the paw is withdrawn from the heat source, the timer is stopped. Mechanical allodynia will be evaluated by paw withdrawal response (PWR) to application of force using von Frey monofilaments. The same tests will be performed at different time points following surgery to quantify the PWL and PWR in order to observe the functional recovery of the severed nerve. A series of pre-operative tests is used for comparison[41].

All experiments using animals are conducted in compliance with NIH guidelines and institutional IACUC approval. General anesthesia is induced with pentobarbital 40 mg/kg IP and supplemented with 2-4 mg/kg as needed to maintain anesthetic depth. Both sciatic nerves are dissected free with microsurgical technique in strict aseptic conditions. A dorsal longitudinal skin incision is made slightly to the left of midline over the pelvic girdle. Slightly caudal and ventral to the left hip joint, a faint separation of muscle groups is visualized. A 10 mm incision is made along the separation of the muscle groups and deepened by blunt

dissection. The sciatic nerve is visualized running parallel to the length of the femur. A 7-10 mm length of the sciatic nerve, proximal to the sciatic trifurcation is carefully cleared from underlying tissue using blunt dissection[153].

The left sciatic nerve is either sutured with 4 sutures at ½ the length from the spinal cord, or transected at 2/3 its length from the spinal cord. The right nerve serves as a control. The scaffolds are placed along the site of injury, or in the case of removal each end of the transected nerve will be inserted into the lumen of the scaffold. The nerve ends will be grafted using fibrin glue. Approximately 5μL of fibrin glue will be applied and allowed to set for 5 minutes. The surgical site is closed using surgical clips, and rats will be allowed to recover from anesthesia under heating lamps prior to return to the animal facility. Cyclosporine A will be administered to rats receiving human cells via gastral gavage to suppress rejection (6 mg/kg/day). This is administered via gavage to reduce the amount of pain and physical trauma to the rat by daily IP injections.

Stem Cell Culture and Maintenance

Undifferentiated male hES cell colonies (grown on a layer of mouse endothelial fibroblasts (MEFs) in hES medium [20% KSR, DMEM/F12, 1% NEAA, 1% L-Glutamine, 0.1mM BME, 4ng/mL FGF-2] in 3% O_2 conditions) are collected under direct vision using a combination of collagenase IV digestion and mechanical disruption, to strip the colonies away from the underlying fibroblast feeder layer. The colonies are allowed to repeatedly sediment and are washed three times, then triturated gently to give a single cell suspension.

For studies with cells more defined than hES cells, a protocol is followed to differentiate hES cells in the CNS cells. Undifferentiated male hES cell colonies grown on a feeder layer of MEFs in hES medium. hES cells are passaged manually (1:2-1:5) following a collagenase

IV treatment. This is repeated every four days up to p80. To begin differentiation of the hES cells, they are detached from the MEF feeder layer using Accutase II treatment, and triturated to a single-cell suspension. This is then transferred to matrigel-coated plates at a density of 10^5cells/cm^2. After 24 hours, the hES medium is replaced with NAA medium [DMEM/F12, 200μM transferin, 20μg/mL insulin, 20nM progesterone, 100μm putrescine, 30mM sodium selenite, 10ng/mL FGF-2]. These cells are then allowed to grow for six days. On day eight, cells are detached using collagenase IV for 20 minutes, detached by gentle scraping. Cells are transferred to bacterial Petri-dishes (3 x 3.5cm into 1 x 10cm) to form neurospheres in 15 days. FGF-2 is added daily via the NAA medium. After 15 days (day 23), the neurospheres are placed onto tissue culture plates for 3 days. After the three day outgrowth of neuro-precursor cells, they are triturated to a single cell suspension and transferred to polyornithine-coated plates (P0; $5x10^6$ cells). These neural progenitor cells are passaged after 3 days.

Preparation of Implants

PGS scaffolds are rinsed in an ethanol wash series (70%, 50%, and 25%) for 30 minutes each, followed by a 30 minute PBS rinse. Scaffolds are then incubated in the culture medium overnight prior to seeding. Following the injection of the cell suspension, the scaffolds are submerged in medium and incubated for 6 hours at 3% O_2. At this point the cells are resuspended by detachment from the MEF layer by collagenase IV treatment, washed 3 times and triturated gently into a single-cell suspension. An aliquot is taken for counting. The cells are suspended in liquid alginate at a density of 500,000 cells per 100μL, of which is then injected through the lumen of the PGS scaffold. The scaffold is then dropped in a barium solution which polymerizes the alginate locking the hES cells in place.

In order to compare the hES cells with the previous literature, the use of Schwann cells in this study is essential. From the point at which the cells are suspended in alginate at the density of 500,000 cells per 100μL into the scaffolds, there will be scaffolds with no cells, hES cells, NPCs, and Schwann cells, with the varying conditions of with/without alginate, and 6% vs. 20% oxygen. By comparing the findings with no cells and Schwann cells to that of the literature, it should be easily determined whether the stem cells or neural progenitor cells are enhancing regeneration or not.

Scaffold Optimization

Nerve regeneration and scaffold degradation will be observed every 10 days. In tact scaffolds are explanted followed by a soak in calcium/barium-free solution to depolymerize the alginate, followed by a 0.25% trypsin treatment to remove any cellular material. Volume is determined by submerging the scaffolds in mercury, measuring displacement. The explants are then dried at 40ºC under vacuum (85mTorr) for 48h. Optimization of scaffold size will depend on the experimental rate of nerve regeneration versus the rate of degradation of the scaffold.

Tissue Processing for Histology

The distal half of the sciatic nerve and proximal half will be separately analyzed with the lesion and scaffold in the distal half. Continuity of the nerve will be noted at autopsy and photos of the gross morphology taken. Nerve samples will be soaked in sterile saline, then fixed in periodate-lysine-paraformaldehyde (PLP) for 30 minutes, then stored in 10% sucrose. The samples are dried in graded alcohols and embedded in paraffin. The midsection, containing the lesion and scaffold will be sectioned in 1μm sections to quantify neural regeneration. In addition, some immunohistochemical assays will be performed to

evaluate the persistence of inflammatory infiltrates and the number of Schwann cells. Sections will be prepared for histology using a cryomicrotome or by paraffin wax embedding.

Histochemistry and Immunohistochemistry

Because the cells implanted are human cells, even differentiated cells will express human alkaline phosphatase (hAP) and human IgG. Schwann Cells are labeled and counted using Anti-S100β. Comparing the Anti-hAP and Anti-IgG labeled cells with the Anti-S100β cells will indicate whether the cells are derived from the stem cells or the native tissue. Tissue slides are fixed in 4% paraformaldehyde (PF) for 5 min and then labeled with the primary and secondary antibodies. Nuclei are counterstained with DAPI[154].

To observe the general anatomy of the nerve, the tissue will be prepared using eosin and hematoxylin staining. If preparations were embedded in paraffin wax, the wax is removed in 2 changes of xylene, soaking 10 minutes each. The samples are rehydrated in 100% ethanol twice for 5 minutes, and then briefly washed. The sample is then stained in hematoxylin for 8 minutes followed by a 5 minute wash in running water. The stain is differentiated in 1% acid alcohol for 30 seconds, and then washed in running water for 30 seconds. Samples are then added to a 0.2 ammonia water solution for 45 seconds followed by another 5 minute running water rinse. They are then dipped in 95% ethanol 10 times before counterstaining in eosin Y solution for 45 seconds. The sample is then dehydrated in 95% ethanol and 2 changes of absolute ethanol for 5 minutes each. This is finished with 2 changes of xylene for 5 minutes each and mounting with a xylene-based mounting medium.

Preparation for SEM begins with immersion of the (paraffin removed) sample in 3% glutaraldehyde for 3 hours followed by 3 x 15 minute washes in buffer. The samples are

post-fixed in osmium tetroxide in buffer for 2 hours. The tissue is dehydrated via a serial wash in ethanol starting with 50% in buffer up to 100% ethanol. Each of the 6 washes is 30 minutes. Samples are dried in a critical point dryer and then transferred to an SEM sample holder. This is then placed in the sputtering device where a heavy metal is sputtered over the entire sample under vacuum. Once the sample is sputtered it can be placed in the SEM chamber, vacuum brought down, and then viewed.

Molecular Biology

The tissue of interest is collected, weighed, and homogenized in 3mL of PBS buffer per gram of tissue, maintaining 4°C throughout. This is incubated for 30 minutes and transferred to microcentrifuge tubes. This slurry then centrifuged at 400g for 10 minutes at 4°C. The supernatant is removed and discarded and tissue is washed again. After the second wash, the supernatant is again removed and tissue is resuspended in 600µL lysis buffer per gram tissue, which contains a protease inhibitor cocktail. The sample is gently vortexed and then placed on ice for a 30 minute incubation with occasional mixing. The lysate is centrifuged at 10,000g for 15 minutes at 4°C. The supernatant is collected and transferred to a clean tube.

50µL of Protein G slurry is transferred to an eppendorf tube along with 450µL of cold lysis Buffer. The beads are centrifuged at 10,000g for 30 seconds and washed again with lysis buffer, and then finally resuspended in 50µL of lysis buffer. This 50µL slurry of Protein G is added to 500µL of cell lysate in a new tube and incubated for 60 minutes. The samples are then spun at 10,000g for 10 minutes at 4°C and the supernatants are collected, being careful not to transfer the beads.

About 5-10μg of antibody for the target protein (NGF, EPO, BDNF, GDNF, etc.) is added to the pre-cleared lysate and incubated for an hour. 50μL of washed Protein G slurry in lysis buffer is then added and the sample is incubated for 1 hour at 4°C on a rotator. The sample is centrifuged at 10,000g for 30 seconds and 4°C. The supernatant is completely collected and the beads are washed 3-5 times with 500μL of lysis buffer. After the last wash, the supernatant is aspirated followed by the addition of 50μL of Laemmli sample buffer to the bead pellet. This is vortexed and heated to 90-100°C for 10 minutes. The samples are again spun at 10,000g for 5 minutes and the supernatant is collected and loaded onto the SDS-polyacrylamide gel. The protocol for running the SDS-PAGE will be per manufacturer. The gel will be incubated in a blocking buffer (5% carnation dry milk in TBST) prior to exposure to the primary antibody, which will be incubated overnight. The gel will be thoroughly washed before incubating in the secondary antibody.

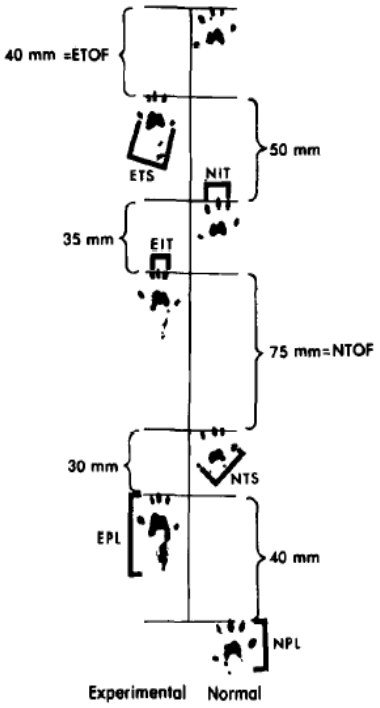

Figure 4: Determination of SFI using ink to track the paw prints of rats before and after nerve injury[38].

Chapter 4

Aims and Procedure for Future Study

In this chapter, I bring forward specific aims for potential continuation of this work. These are presented in the final chapter because none of the aims were fully completed, however, if future studies continue with this research, the following aims may set a guideline as to how to continue.

Aim 1: Optimize the scaffolds to deliver embedded stem cells and provide mechanical support of the recovering nerve

The ***working hypothesis*** is that physical and chemical properties affect the performance of the hydrogel and scaffold *in vivo*. Physical parameters of the scaffold to be optimized include the pore size, porosity, and physical size of the scaffold itself. The cross-linking density controls the hydrophobicity of PGS, and thus the adsorption of various important ECM proteins. The concentration of alginate will be adjusted to optimize the release of neural growth factors such as Epo, BDNF, GDNF, or NGF while the viscosity must be optimized for delivery into the porous scaffold. This study will begin *in vitro* to optimize the seeding and implantation of the stem cells and Schwann cells followed by a further optimization *in vivo*, using data obtained as feedback for degradation rates and regeneration rate. Success *in vitro* will be determined by maintenance of the stem cells and Schwann cells within the gel/scaffold in culture for 2 weeks. The gel is broken down releasing the cells, which will then be quantified in number and viability. If the cells are viable and still remain, then optimization of the scaffold *in vivo* will resume. **Success *in vivo* will be demonstrated by sufficient support (and not interference) of the scaffold**

throughout the healing process and communication of the seeded cells with the endogenous system.

Aim 2: Evaluate the ability of the scaffolds to reverse neuropathic pain induced by Chronic Constriction Injury

The ***working hypothesis*** is that the human embryonic stem (hES) cell or neural progenitor cell (NPC)-seeded implants will better recover the **chronic constriction injury (CCI)** than Schwann cells or without cells by faster reducing the neuropathic pain. A ***secondary hypothesis*** predicts that the implant will yield a minimal immune response, as well as have no significant effect on the sciatic nerve or behavior of the rats. Behavioral tests analyzing the rats' responses to calibrated thermal and mechanical stimuli will be performed daily to quantify neuropathic pain. Neuropathic pain will be confirmed with significant hypersensitivity to the stimuli. Rats will be euthanized at different times from 0 day to 90 days to observe the healing and degradation of the polymers. The site of surgery will be examined pathologically, histologically, and by immunostaining following euthanization. **Success will be defined by the recovery of behavioral function without neuropathic pain in correlation with appropriate physiology of the site of injury.** Furthermore, the suppression of teratoma formation is essential for the efficacy of this procedure. Histology and immunochemistry will be used to determine the origin of the cells and tissues present in different regions of the lesion.

Aim 3: Examine the recovery from neuropathic pain with scaffold implantation following Autologous Nerve Grafting

My ***working hypothesis*** is that the implant seeded with hES or NPCs will better recover the potential neuropathic pain resulting from **autologous nerve grafting** than without cells or Schwann cells. Preparation of the scaffolds is same as in Aims 1 and 2.

Behavioral tests will be performed daily to assess any neuropathic pain. Rats will be euthanized at different times for further analysis as performed in Aim 2. **The success of this aim will be shown with improved behavioral recovery as quantified by observation of the gait of rats post operatively as well as the recovery from neuropathic pain as demonstrated by the thermal and mechanical stimuli testing.**

Aim 4: Compare the neuroregenerative potential of young vs. aged rats

It is known that there is a decline of regenerative potential of peripheral nerves with age. The ***working hypothesis*** of this aim is that the use of the optimized seeded scaffold will recover the aged rats in a time frame similar to the young rats. This will be analyzed comparing young rats (<3mo.) with aged rats (>8mo.) performing the chronic constriction injuries and autografting techniques as in previous experiments. Results will be analyzed by functional recovery and presence of neuropathic pain. **Success will be based on the ability of the scaffolds to aid in complete recovery of aged rats in a time frame similar to the young rats.**

Aim 5: Compare the neuroregenerative potential of superoxide dismutase knockout rats

Superoxide dismutase is directly related to the oxidative damage imposed on the cell, thus the ***working hypothesis*** is that the use of the optimized ES cell-seeded scaffold will provide an environment that induces an endogenous response that will recover the damaged nerve. Rats that will be compared will include homozygous Sod1 (-/-) (Cu, Zn-SOD), heterozygous Sod2 (+/-) (Mn-SOD), and homozygous GPx1 (-/-). Both injury models will be tested with the aforementioned varying conditions. Results will be analyzed based on functional recovery as well as presence of neuropathic pain. **Success of this aim will be**

the creation of a model that can link the common growth factors, common aging factors, the decline in neural potential, and a possible mechanism to surpass aging deficiencies.

Discussion

The cumulative studies as described in these five aims both reflect and penetrate into the topics initially discussed: the problems of neuropathic pain, a method to potentially reduce or reverse neuropathic pain, the notion that neural regeneration declines with age, and the capacity of a cell-infused implant to aid in neural regeneration and reconstruction in both cases of injured and severed nerves.

Aim 1 explores the capacity of the implant to guide nerve repair using different types of cells, NPCs, hES cells, and Schwann cells to repair the nerve *in vivo*. The ultimate goal of this aim will be based on feedback and alteration of the physical properties of the biomaterial scaffold as well as the concentration of cells delivered to the site of injury. Schwann cells are included to compare with existing studies that have only used Schwann cells in NGCs[102, 103, 109, 115].

While there is still some controversy in whether these experiments using a transected sciatic nerve from rat is even significant, a more established model is used to explore the effects on neuropathic pain in Aim 2. Furthermore, the incidence of chronic neuropathic pain is much higher in the CCI model than in nerve transection. Aim 2 follows the standard protocols of Bennett and Xie[38] to explore the different symptoms of neuropathic pain, and then examines these symptoms following implantation of the seeded scaffold. This Aim more clearly examines the aspect of pain whereas Aim 3 is more focused on the regenerative potential of the scaffolds.

Like Aim 2, Aim 3 utilizes the optimized scaffold from Aim 1 and applies it to the sciatic transection model, observing the recovery from this injury. This is compared both to natural recovery as well as with the standard medical procedure in such cases, which is autologous nerve grafting. Similar to the tests in Aim 2, the rats in this study will be examined for neuropathic pain and subsequent recovery. As mentioned above, the incidence of pain is less with neural transection than with CCI. Furthermore, this study should be continued with a larger animal such as a rabbit, where a full 15mm section of the sciatic nerve can be removed and watched for recovery as there is some controversy as to whether 10-12mm sections in rats are long enough for significant results.

Aims 4 and 5 both explore the process of aging. With aging, it is known that both recovery of function and loss of pain come at a much slower rate if at all. Aim 4 compares the studies explored in Aims 2 and 3 amongst young and old rats to confirm this reduced healing potential as well as to observe how the implant can affect the rates of recovery and reversal of neuropathic pain. Aim 5 explores deeper into one potential cause of cellular aging, free oxygen radical damage.

In order to explore how oxygen radical damage affects the body, of knockout rats for the enzymes that reduce the free oxygen radicals will be used to simulate aging. Characteristics of these rats will be documented before the procedures employed in Aims 2 and 3 will again be used. Once accomplished, the data from Aim 5 will be compared to that of Aim 4 to cross-examine the model for aging with actual aged rats.

All of the Aims, while separate, all drive to answer a set of questions posed in the Introduction. Aim 1 is the driving step in this research, and provides the optimized scaffold for delivery of the cells that are hypothesized to aid in the neuroregenerative process. Aims 2 and 3 lay down the foundation for the experimental procedures that will be used to obtain

the data of regenerative potential, functional recovery, as well as recovery from neuropathic pain. Aims 4 and 5 push beyond the initial studies and examine how aging negatively affects neural regeneration and whether oxidative stress is the cause of this and whether this implant can restore the lost or lagging neural potential, and drive even an elderly nerve to full recovery.

References

1. Divers, T.J. Acquired spinal cord and peripheral nerve disease. *Vet. Clin. North Am. Food Anim. Pract.* 20, 231-242, v-vi (2004).

2. Eichberg, J. & Zhu, X. Diacylglycerol composition and metabolism in peripheral nerve. *Adv. Exp. Med. Biol.* 318, 413-425 (1992).

3. Kennedy, J.M. & Zochodne, D.W. Impaired peripheral nerve regeneration in diabetes mellitus. *J. Peripher. Nerv. Syst.* 10, 144-157 (2005).

4. Mackinnon, S.E., Hudson, A.R., Gentili, F., Kline, D.G. & Hunter, D. Peripheral nerve injection injury with steroid agents. *Plast. Reconstr. Surg.* 69, 482-490 (1982).

5. Nickell, K. & Boone, T.B. Peripheral neuropathy and peripheral nerve injury. *Urol. Clin. North Am.* 23, 491-500 (1996).

6. Saray, A., Apan, A. & Kisa, U. Free radical-induced damage in experimental peripheral nerve injection injury. *J. Reconstr. Microsurg.* 19, 401-406 (2003).

7. Strasberg, J.E. et al. Peripheral nerve injection injury with antiemetic agents. *J. Neurotrauma* 16, 99-107 (1999).

8. Streit, W.J. & Kreutzberg, G.W. Response of endogenous glial cells to motor neuron degeneration induced by toxic ricin. *J. Comp. Neurol.* 268, 248-263 (1988).

9. Soreide, A.J. Variations in the axon reaction in animals of different ages. A light microscopic study on the facial nucleus of the rat. *Acta Anat. (Basel)* 110, 40-47 (1981).

10. Tanaka, K. & Webster, H.D. Myelinated fiber regeneration after crush injury is retarded in sciatic nerves of aging mice. *J. Comp. Neurol.* 308, 180-187 (1991).

11. Tanaka, K., Zhang, Q.L. & Webster, H.D. Myelinated fiber regeneration after sciatic nerve crush: morphometric observations in young adult and aging mice and the effects of macrophage suppression and conditioning lesions. *Exp. Neurol.* 118, 53-61 (1992).

12. Vaughan, D.W. Effects of advancing age on peripheral nerve regeneration. *J. Comp. Neurol.* 323, 219-237 (1992).

13. Kawabuchi, M., Chongjian, Z., Islam, A.T., Hirata, K. & Nada, O. The effect of aging on the morphological nerve changes during muscle reinnervation after nerve crush. *Restor. Neurol. Neurosci.* 13, 117-127 (1998).

14. Streppel, M. et al. Slow axonal regrowth but extreme hyperinnervation of target muscle after suture of the facial nerve in aged rats. *Neurobiol. Aging* 19, 83-88 (1998).

15. Verdu, E., Ceballos, D., Vilches, J.J. & Navarro, X. Influence of aging on peripheral nerve function and regeneration. *J. Peripher. Nerv. Syst.* 5, 191-208 (2000).

16. Shin, S., Dalton, S. & Stice, S.L. Human motor neuron differentiation from human embryonic stem cells. *Stem Cells Dev.* 14, 266-269 (2005).

17. Glass, J.D. Wallerian degeneration as a window to peripheral neuropathy. *J Neurol Sci* 220, 123-124 (2004).

18. Williams, P.L. & Hall, S.M. Chronic Wallerian degeneration--an in vivo and ultrastructural study. *J. Anat.* 109, 487-503 (1971).

19. Stoll, G., Griffin, J.W., Li, C.Y. & Trapp, B.D. Wallerian degeneration in the peripheral nervous system: participation of both Schwann cells and macrophages in myelin degradation. *J. Neurocytol.* 18, 671-683 (1989).

20. Fenrich, K. & Gordon, T. Canadian Association of Neuroscience review: axonal regeneration in the peripheral and central nervous systems--current issues and advances. *Can J Neurol Sci* 31, 142-156 (2004).

21. Li, X., Gonias, S.L. & Campana, W.M. Schwann cells express erythropoietin receptor and represent a major target for Epo in peripheral nerve injury. *Glia* 51, 254-265 (2005).

22. Schlaepfer, W.W. & Bunge, R.P. Effects of calcium ion concentration on the degeneration of amputated axons in tissue culture. *J Cell Biol* 59, 456-470 (1973).

23. George, E.B., Glass, J.D. & Griffin, J.W. Axotomy-induced axonal degeneration is mediated by calcium influx through ion-specific channels. *J Neurosci* 15, 6445-6452 (1995).

24. Stoll, G., Jander, S. & Myers, R.R. Degeneration and regeneration of the peripheral nervous system: from Augustus Waller's observations to neuroinflammation. *J Peripher Nerv Syst* 7, 13-27 (2002).

25. Sumner, A.J. Aberrant reinnervation. *Muscle Nerve* 13, 801-803 (1990).

26. English, A.W. Enhancing axon regeneration in peripheral nerves also increases functionally inappropriate reinnervation of targets. *J. Comp. Neurol.* 490, 427-441 (2005).

27. Robinson, I. & Meert, T.F. Stability of neuropathic pain symptoms in partial sciatic nerve ligation in rats is affected by suture material. *Neurosci. Lett.* 373, 125-129 (2005).

28. Siren, A.L. et al. Erythropoietin prevents neuronal apoptosis after cerebral ischemia and metabolic stress. *Proc Natl Acad Sci U S A* 98, 4044-4049 (2001).

29. Sekiguchi, Y., Kikuchi, S., Myers, R.R. & Campana, W.M. ISSLS prize winner: Erythropoietin inhibits spinal neuronal apoptosis and pain following nerve root crush. *Spine* 28, 2577-2584 (2003).

30. Digicaylioglu, M. & Lipton, S.A. Erythropoietin-mediated neuroprotection involves cross-talk between Jak2 and NF-kappaB signalling cascades. *Nature* 412, 641-647 (2001).

31. Csete, M., Rodriguez, L., Wilcox, M. & Chadalavada, S. Erythropoietin receptor is expressed on adult rat dopaminergic neurons and erythropoietin is neurotrophic in cultured dopaminergic neuroblasts. *Neurosci. Lett.* 359, 124-126 (2004).

32. Campana, W.M. & Myers, R.R. Exogenous erythropoietin protects against dorsal root ganglion apoptosis and pain following peripheral nerve injury. *Eur J Neurosci* 18, 1497-1506 (2003).

33. Angelov, D.N., Gunkel, A., Stennert, E. & Neiss, W.F. Recovery of original nerve supply after hypoglossal-facial anastomosis causes permanent motor hyperinnervation of the whisker-pad muscles in the rat. *J Comp Neurol* 338, 214-224 (1993).

34. Valero-Cabre, A., Tsironis, K., Skouras, E., Navarro, X. & Neiss, W.F. Peripheral and spinal motor reorganization after nerve injury and repair. *J Neurotrauma* 21, 95-108 (2004).

35. Jensen, T.S., Gottrup, H., Sindrup, S.H. & Bach, F.W. The clinical picture of neuropathic pain. *Eur J Pharmacol* 429, 1-11 (2001).

36. Boucher, T.J. & McMahon, S.B. Neurotrophic factors and neuropathic pain. *Curr Opin Pharmacol* 1, 66-72 (2001).

37. Woolf, C.J. & Mannion, R.J. Neuropathic pain: aetiology, symptoms, mechanisms, and management. *Lancet* 353, 1959-1964 (1999).

38. Bennett, G.J. & Xie, Y.K. A peripheral mononeuropathy in rat that produces disorders of pain sensation like those seen in man. *Pain* 33, 87-107 (1988).

39. Ossipov, M.H. & Porreca, F. Challenges in the development of novel treatment strategies for neuropathic pain. *NeuroRx* 2, 650-661 (2005).

40. Irving, G.A. Contemporary assessment and management of neuropathic pain. *Neurology* 64, S21-27 (2005).

41. Klass, M., Hord, A., Wilcox, M., Denson, D. & Csete, M. A role for endothelin in neuropathic pain after chronic constriction injury of the sciatic nerve. *Anesth. Analg.* 101, 1757-1762 (2005).

42. Khodorova, A. et al. Endothelin-B receptor activation triggers an endogenous analgesic cascade at sites of peripheral injury. *Nat Med* 9, 1055-1061 (2003).

43. Chiba, S., Iwasaki, Y., Sekino, H. & Suzuki, N. Transplantation of motoneuron-enriched neural cells derived from mouse embryonic stem cells improves motor function of hemiplegic mice. *Cell Transplant* 12, 457-468 (2003).

44. Baamonde, A. et al. Involvement of endogenous endothelins in thermal and mechanical inflammatory hyperalgesia in mice. *Naunyn Schmiedebergs Arch Pharmacol* 369, 245-251 (2004).

45. Weiner, D.K. & Hanlon, J.T. Pain in nursing home residents: management strategies. *Drugs Aging* 18, 13-29 (2001).

46. Cleary, J.F. & Carbone, P.P. Palliative medicine in the elderly. *Cancer* 80, 1335-1347 (1997).

47. Melding, P.S. Is there such a thing as geriatric pain? *Pain* 46, 119-121 (1991).

48. Khalil, Z., Liu, T. & Helme, R.D. Free radicals contribute to the reduction in peripheral vascular responses and the maintenance of thermal hyperalgesia in rats with chronic constriction injury. *Pain* 79, 31-37 (1999).

49. Dray, A. Inflammatory mediators of pain. *Br J Anaesth* 75, 125-131 (1995).

50. Semsei, I., Rao, G. & Richardson, A. Expression of superoxide dismutase and catalase in rat brain as a function of age. *Mech Ageing Dev* 58, 13-19 (1991).

51. Wagner, R., Heckman, H.M. & Myers, R.R. Wallerian degeneration and hyperalgesia after peripheral nerve injury are glutathione-dependent. *Pain* 77, 173-179 (1998).

52. Novak, J.C. et al. Aging and neuropathic pain. *Brain Res* 833, 308-310 (1999).

53. Crisp, T. et al. Aging, peripheral nerve injury and nociception: effects of the antioxidant 16-desmethyltirilazad. *Behav Brain Res* 166, 159-165 (2006).

54. Medders, G., Mattox, D.E. & Lyles, A. Effects of fibrin glue on rat facial nerve regeneration. *Otolaryngol. Head Neck Surg.* 100, 106-109 (1989).

55. Dagum, A.B. Peripheral nerve regeneration, repair, and grafting. *J. Hand Ther.* 11, 111-117 (1998).

56. Detweiler, M.B., Detweiler, J.G. & Fenton, J. Sutureless and reduced suture anastomosis of hollow vessels with fibrin glue: a review. *J. Invest. Surg.* 12, 245-262 (1999).

57. Choi, B.H. et al. Autologous fibrin glue in peripheral nerve regeneration in vivo. *Microsurgery* 25, 495-499 (2005).

58. Martins, R.S., Siqueira, M.G., Silva, C.F., Godoy, B.O. & Plese, J.P. Electrophysiologic assessment of regeneration in rat sciatic nerve repair using

suture, fibrin glue or a combination of both techniques. *Arq. Neuropsiquiatr.* 63, 601-604 (2005).

59. Martins, R.S., Siqueira, M.G., Da Silva, C.F. & Plese, J.P. Overall assessment of regeneration in peripheral nerve lesion repair using fibrin glue, suture, or a combination of the 2 techniques in a rat model. Which is the ideal choice? *Surg Neurol* 64 Suppl 1, S1:10-16; discussion S11:16 (2005).

60. Hadlock, T. et al. A novel, biodegradable polymer conduit delivers neurotrophins and promotes nerve regeneration. *Laryngoscope* 109, 1412-1416 (1999).

61. Evans, G.R. et al. Clinical long-term in vivo evaluation of poly(L-lactic acid) porous conduits for peripheral nerve regeneration. *J. Biomater. Sci. Polym. Ed.* 11, 869-878 (2000).

62. Hadlock, T., Sundback, C., Hunter, D., Cheney, M. & Vacanti, J.P. A polymer foam conduit seeded with Schwann cells promotes guided peripheral nerve regeneration. *Tissue Eng.* 6, 119-127 (2000).

63. Rosner, B.I., Siegel, R.A., Grosberg, A. & Tranquillo, R.T. Rational design of contact guiding, neurotrophic matrices for peripheral nerve regeneration. *Ann. Biomed. Eng.* 31, 1383-1401 (2003).

64. Hou, S.Y., Zhang, H.Y., Quan, D.P., Liu, X.L. & Zhu, J.K. Tissue-engineered peripheral nerve grafting by differentiated bone marrow stromal cells. *Neuroscience* 140, 101-110 (2006).

65. Giardino, R. et al. Biological and synthetic conduits in peripheral nerve repair: a comparative experimental study. *Int. J. Artif. Organs* 18, 225-230 (1995).

66. Giardino, R., Fini, M., Nicoli Aldini, N., Giavaresi, G. & Rocca, M. Polylactide bioabsorbable polymers for guided tissue regeneration. *J. Trauma* 47, 303-308 (1999).

67. Aldini, N.N. et al. [Trauma of the peripheral nervous system: experimental assessments with guided tissue regeneration]. *Acta Biomed. Ateneo. Parmense.* 70, 49-55 (1999).

68. Wan, A.C. et al. Fabrication of poly(phosphoester) nerve guides by immersion precipitation and the control of porosity. *Biomaterials* 22, 1147-1156 (2001).

69. Xu, X. et al. Peripheral nerve regeneration with sustained release of poly(phosphoester) microencapsulated nerve growth factor within nerve guide conduits. *Biomaterials* 24, 2405-2412 (2003).

70. Evans, G.R. et al. In vivo evaluation of poly(L-lactic acid) porous conduits for peripheral nerve regeneration. *Biomaterials* 20, 1109-1115 (1999).

71. Patist, C.M. et al. Freeze-dried poly(D,L-lactic acid) macroporous guidance scaffolds impregnated with brain-derived neurotrophic factor in the transected adult rat thoracic spinal cord. *Biomaterials* 25, 1569-1582 (2004).

72. Mligiliche, N.L., Tabata, Y. & Ide, C. Nerve regeneration through biodegradable gelatin conduits in mice. *East Afr. Med. J.* 76, 400-406 (1999).

73. Platt, C.I., Krekoski, C.A., Ward, R.V., Edwards, D.R. & Gavrilovic, J. Extracellular matrix and matrix metalloproteinases in sciatic nerve. *J. Neurosci. Res.* 74, 417-429 (2003).

74. Gamez, E. et al. Photofabricated gelatin-based nerve conduits: nerve tissue regeneration potentials. *Cell Transplant.* 13, 549-564 (2004).

75. Cheng, M. et al. Studies on nerve cell affinity of biodegradable modified chitosan films. *J. Biomater. Sci. Polym. Ed.* 14, 1155-1167 (2003).

76. Rosales-Cortes, M. et al. [Regeneration of the axotomised sciatic nerve in dogs using the tubulisation technique with Chitosan biomaterial preloaded with progesterone]. *Rev. Neurol.* 36, 1137-1141 (2003).

77. Yuan, Y., Zhang, P., Yang, Y., Wang, X. & Gu, X. The interaction of Schwann cells with chitosan membranes and fibers in vitro. *Biomaterials* 25, 4273-4278 (2004).

78. B, B.T., Gao, S., Wang, S. & Ramakrishna, S. Development of fibrous biodegradable polymer conduits for guided nerve regeneration. *J. Mater. Sci. Mater. Med.* 16, 367-375 (2005).

79. Cao, W. et al. Physical, mechanical and degradation properties, and schwann cell affinity of cross-linked chitosan films. *J. Biomater. Sci. Polym. Ed.* 16, 791-807 (2005).

80. Chavez-Delgado, M.E. et al. Ultrastructural analysis of guided nerve regeneration using progesterone- and pregnenolone-loaded chitosan prostheses. *J. Biomed. Mater. Res. B. Appl. Biomater.* 74, 589-600 (2005).

81. Freier, T., Montenegro, R., Shan Koh, H. & Shoichet, M.S. Chitin-based tubes for tissue engineering in the nervous system. *Biomaterials* 26, 4624-4632 (2005).

82. Huang, Y.C., Huang, Y.Y., Huang, C.C. & Liu, H.C. Manufacture of porous polymer nerve conduits through a lyophilizing and wire-heating process. *J. Biomed. Mater. Res. B. Appl. Biomater.* 74, 659-664 (2005).

83. Guenard, V., Kleitman, N., Morrissey, T.K., Bunge, R.P. & Aebischer, P. Syngeneic Schwann cells derived from adult nerves seeded in semipermeable guidance channels enhance peripheral nerve regeneration. *J. Neurosci.* 12, 3310-3320 (1992).

84. Bellamkonda, R., Ranieri, J.P., Bouche, N. & Aebischer, P. Hydrogel-based three-dimensional matrix for neural cells. *J. Biomed. Mater. Res.* 29, 663-671 (1995).

85. Dillon, G.P., Yu, X., Sridharan, A., Ranieri, J.P. & Bellamkonda, R.V. The influence of physical structure and charge on neurite extension in a 3D hydrogel scaffold. *J. Biomater. Sci. Polym. Ed.* 9, 1049-1069 (1998).

86. Yu, X., Dillon, G.P. & Bellamkonda, R.B. A laminin and nerve growth factor-laden three-dimensional scaffold for enhanced neurite extension. *Tissue Eng.* 5, 291-304 (1999).

87. Plant, G.W., Chirila, T.V. & Harvey, A.R. Implantation of collagen IV/poly(2-hydroxyethyl methacrylate) hydrogels containing Schwann cells into the lesioned rat optic tract. *Cell Transplant.* 7, 381-391 (1998).

88. Lesny, P. et al. Polymer hydrogels usable for nervous tissue repair. *J. Chem. Neuroanat.* 23, 243-247 (2002).

89. Mosahebi, A., Wiberg, M. & Terenghi, G. Addition of fibronectin to alginate matrix improves peripheral nerve regeneration in tissue-engineered conduits. *Tissue Eng.* 9, 209-218 (2003).

90. Novikova, L.N. et al. Alginate hydrogel and matrigel as potential cell carriers for neurotransplantation. *J. Biomed. Mater. Res. A.* (2006).

91. Novikov, L.N. et al. A novel biodegradable implant for neuronal rescue and regeneration after spinal cord injury. *Biomaterials* 23, 3369-3376 (2002).

92. Flynn, L., Dalton, P.D. & Shoichet, M.S. Fiber templating of poly(2-hydroxyethyl methacrylate) for neural tissue engineering. *Biomaterials* 24, 4265-4272 (2003).

93. Midha, R., Munro, C.A., Dalton, P.D., Tator, C.H. & Shoichet, M.S. Growth factor enhancement of peripheral nerve regeneration through a novel synthetic hydrogel tube. *J Neurosurg* 99, 555-565 (2003).

94. Mohanna, P.N., Young, R.C., Wiberg, M. & Terenghi, G. A composite poly-hydroxybutyrate-glial growth factor conduit for long nerve gap repairs. *J. Anat.* 203, 553-565 (2003).

95. Belkas, J.S., Munro, C.A., Shoichet, M.S. & Midha, R. Peripheral nerve regeneration through a synthetic hydrogel nerve tube. *Restor. Neurol. Neurosci.* 23, 19-29 (2005).

96. Wang, W., Fan, M., Zhi, X.D., Liu, S.H. & Liu, P.D. [Repair of peripheral nerve gap with the use of tissue engineering scaffold complex]. *Zhongguo. Yi. Xue. Ke. Xue. Yuan. Xue. Bao.* 27, 688-691 (2005).

97. Jain, A., Kim, Y.T., McKeon, R.J. & Bellamkonda, R.V. In situ gelling hydrogels for conformal repair of spinal cord defects, and local delivery of BDNF after spinal cord injury. *Biomaterials* 27, 497-504 (2006).

98. Katayama, Y. et al. Coil-reinforced hydrogel tubes promote nerve regeneration equivalent to that of nerve autografts. *Biomaterials* 27, 505-518 (2006).

99. Schmidt, C.E. & Leach, J.B. Neural tissue engineering: strategies for repair and regeneration. *Annu. Rev. Biomed. Eng.* 5, 293-347 (2003).

100. Rosso, F. et al. Smart materials as scaffolds for tissue engineering. *J. Cell Physiol.* 203, 465-470 (2005).

101. Borkenhagen, M., Stoll, R.C., Neuenschwander, P., Suter, U.W. & Aebischer, P. In vivo performance of a new biodegradable polyester urethane system used as a nerve guidance channel. *Biomaterials* 19, 2155-2165 (1998).

102. Cai, J., Peng, X., Nelson, K.D., Eberhart, R. & Smith, G.M. Permeable guidance channels containing microfilament scaffolds enhance axon growth and maturation. *J. Biomed. Mater. Res. A.* (2005).

103. Schmalenberg, K.E. & Uhrich, K.E. Micropatterned polymer substrates control alignment of proliferating Schwann cells to direct neuronal regeneration. *Biomaterials* 26, 1423-1430 (2005).

104. Levi, A.D., Guenard, V., Aebischer, P. & Bunge, R.P. The functional characteristics of Schwann cells cultured from human peripheral nerve after transplantation into a gap within the rat sciatic nerve. *J. Neurosci.* 14, 1309-1319 (1994).

105. Fansa, H., Keilhoff, G., Wolf, G., Schneider, W. & Gold, B.G. Tissue Engineering of Peripheral Nerves: A Comparison of Venous and Acellular Muscle Grafts with Cultured Schwann Cells. *Plast. Reconstr. Surg.* 107, 495-496 (2001).

106. Mosahebi, A., Fuller, P., Wiberg, M. & Terenghi, G. Effect of allogeneic Schwann cell transplantation on peripheral nerve regeneration. *Exp. Neurol.* 173, 213-223 (2002).

107. Rutkowski, G.E. & Heath, C.A. Development of a bioartificial nerve graft. II. Nerve regeneration in vitro. *Biotechnol. Prog.* 18, 373-379 (2002).

108. Rutkowski, G.E. & Heath, C.A. Development of a bioartificial nerve graft. I. Design based on a reaction-diffusion model. *Biotechnol. Prog.* 18, 362-372 (2002).

109. Rutkowski, G.E., Miller, C.A., Jeftinija, S. & Mallapragada, S.K. Synergistic effects of micropatterned biodegradable conduits and Schwann cells on sciatic nerve regeneration. *J. Neural. Eng.* 1, 151-157 (2004).

110. Akassoglou, K., Akpinar, P., Murray, S. & Strickland, S. Fibrin is a regulator of Schwann cell migration after sciatic nerve injury in mice. *Neurosci. Lett.* 338, 185-188 (2003).

111. Fansa, H., Dodic, T., Wolf, G., Schneider, W. & Keilhoff, G. Tissue engineering of peripheral nerves: Epineurial grafts with application of cultured Schwann cells. *Microsurgery* 23, 72-77 (2003).

112. May, F. et al. [Nerve repair strategies for restoration of erectile function after radical pelvic surgery]. *Urologe. A.* 44, 780-784 (2005).

113. Belkas, J.S., Shoichet, M.S. & Midha, R. Peripheral nerve regeneration through guidance tubes. *Neurol. Res.* 26, 151-160 (2004).

114. Berger, A. & Lassner, F. Peripheral nerve allografts: survey of present state in an experimental model of the rat. *Microsurgery* 15, 773-777 (1994).

115. Ansselin, A.D., Fink, T. & Davey, D.F. Peripheral nerve regeneration through nerve guides seeded with adult Schwann cells. *Neuropathol Appl Neurobiol* 23, 387-398 (1997).

116. Sundback, C.A. et al. Biocompatibility analysis of poly(glycerol sebacate) as a nerve guide material. *Biomaterials* 26, 5454-5464 (2005).

117. Wang, Y., Ameer, G.A., Sheppard, B.J. & Langer, R. A tough biodegradable elastomer. *Nat. Biotechnol.* 20, 602-606 (2002).

118. Wang, Y., Kim, Y.M. & Langer, R. In vivo degradation characteristics of poly(glycerol sebacate). *J. Biomed. Mater. Res. A.* 66, 192-197 (2003).

119. Rydevik, B.L. et al. An in vitro mechanical and histological study of acute stretching on rabbit tibial nerve. *J. Orthop. Res.* 8, 694-701 (1990).

120. Fidkowski, C. et al. Endothelialized microvasculature based on a biodegradable elastomer. *Tissue Eng.* 11, 302-309 (2005).

121. Yoon, D.M., Hawkins, E.C., Francke-Carroll, S. & Fisher, J.P. Effect of construct properties on encapsulated chondrocyte expression of insulin-like growth factor-1. *Biomaterials* 28, 299-306 (2007).

122. Dikovsky, D., Bianco-Peled, H. & Seliktar, D. The effect of structural alterations of PEG-fibrinogen hydrogel scaffolds on 3-D cellular morphology and cellular migration. *Biomaterials* 27, 1496-1506 (2006).

123. Fansa, H., Keilhoff, G., Wolf, G. & Schneider, W. [Cultivating human Schwann cells for tissue engineering of peripheral nerves]. *Handchir. Mikrochir. Plast. Chir.* 32, 181-186 (2000).

124. Bender, M.D., Bennett, J.M., Waddell, R.L., Doctor, J.S. & Marra, K.G. Multi-channeled biodegradable polymer/CultiSpher composite nerve guides. *Biomaterials* 25, 1269-1278 (2004).

125. Zhang, P. et al. Bridging small-gap peripheral nerve defects using biodegradable chitin conduits with cultured schwann and bone marrow stromal cells in rats. *J. Reconstr. Microsurg.* 21, 565-571 (2005).

126. Klinge, P.M. et al. Regeneration of a transected peripheral nerve by transplantation of spinal cord encapsulated in a vein. *Neuroreport* 12, 1271-1275 (2001).

127. Baez, J.C. et al. Embryonic cerebral cortex cells retain CNS phenotypes after transplantation into peripheral nerve. *Exp. Neurol.* 189, 422-425 (2004).

128. Geuna, S. Embryonic cell grafting for the treatment of peripheral nervous system diseases. *Neuroreport* 12, A101-A102 (2001).

129. Strubing, C. et al. Differentiation of pluripotent embryonic stem cells into the neuronal lineage in vitro gives rise to mature inhibitory and excitatory neurons. *Mech Dev* 53, 275-287 (1995).

130. Bain, G. & Gottlieb, D.I. Neural cells derived by in vitro differentiation of P19 and embryonic stem cells. *Perspect Dev Neurobiol* 5, 175-178 (1998).

131. Bain, G., Kitchens, D., Yao, M., Huettner, J.E. & Gottlieb, D.I. Embryonic stem cells express neuronal properties in vitro. *Dev Biol* 168, 342-357 (1995).

132. Bain, G., Ray, W.J., Yao, M. & Gottlieb, D.I. Retinoic acid promotes neural and represses mesodermal gene expression in mouse embryonic stem cells in culture. *Biochem Biophys Res Commun* 223, 691-694 (1996).

133. Kokai, L.E., Rubin, J.P. & Marra, K.G. The potential of adipose-derived adult stem cells as a source of neuronal progenitor cells. *Plast Reconstr Surg* 116, 1453-1460 (2005).

134. Dezawa, M. et al. Specific induction of neuronal cells from bone marrow stromal cells and application for autologous transplantation. *J Clin Invest* 113, 1701-1710 (2004).

135. Gottlieb, D.I. Large-scale sources of neural stem cells. *Annu Rev Neurosci* 25, 381-407 (2002).

136. Myckatyn, T.M., Mackinnon, S.E. & McDonald, J.W. Stem cell transplantation and other novel techniques for promoting recovery from spinal cord injury. *Transpl. Immunol.* 12, 343-358 (2004).

137. MacDonald, S.C. et al. Functional motor neurons differentiating from mouse multipotent spinal cord precursor cells in culture and after transplantation into transected sciatic nerve. *J. Neurosurg.* 98, 1094-1103 (2003).

138. Harper, J.M. et al. Axonal growth of embryonic stem cell-derived motoneurons in vitro and in motoneuron-injured adult rats. *Proc. Natl. Acad. Sci. U.S.A.* 101, 7123-7128 (2004).

139. Ikeda, R. et al. Transplantation of motoneurons derived from MASH1-transfected mouse ES cells reconstitutes neural networks and improves motor function in hemiplegic mice. *Exp. Neurol.* 189, 280-292 (2004).

140. Gao, J., Coggeshall, R.E., Tarasenko, Y.I. & Wu, P. Human neural stem cell-derived cholinergic neurons innervate muscle in motoneuron deficient adult rats. *Neuroscience* 131, 257-262 (2005).

141. Li, X.J. et al. Specification of motoneurons from human embryonic stem cells. *Nat. Biotechnol.* 23, 215-221 (2005).

142. Hamada, M. et al. Introduction of the MASH1 gene into mouse embryonic stem cells leads to differentiation of motoneuron precursors lacking Nogo receptor expression

that can be applicable for transplantation to spinal cord injury. ***Neurobiol. Dis.*** (2006).

143. Choi, B.H. et al. Transplantation of cultured bone marrow stromal cells to improve peripheral nerve regeneration. ***Int. J. Oral. Maxillofac. Surg.*** 34, 537-542 (2005).

144. Zhang, Y., Lin, H.K., Frimberger, D., Epstein, R.B. & Kropp, B.P. Growth of bone marrow stromal cells on small intestinal submucosa: an alternative cell source for tissue engineered bladder. ***BJU Int.*** 96, 1120-1125 (2005).

145. Chen, X. et al. Study of in vivo differentiation of rat bone marrow stromal cells into schwann cell-like cells. ***Microsurgery*** 26, 111-115 (2006).

146. Pereira Lopes, F.R. et al. Bone marrow stromal cells and resorbable collagen guidance tubes enhance sciatic nerve regeneration in mice. ***Exp. Neurol.*** (2006).

147. Murphy, W.L., Dennis, R.G., Kileny, J.L. & Mooney, D.J. Salt fusion: an approach to improve pore interconnectivity within tissue engineering scaffolds. ***Tissue Eng.*** 8, 43-52 (2002).

148. Crapo, P.M., Gao, J. & Wang, Y. Seamless tubular poly(glycerol sebacate) scaffolds: High-yield fabrication and potential applications. ***J Biomed Mater Res A*** (2007).

149. Gao, J., Crapo, P.M. & Wang, Y. Macroporous elastomeric scaffolds with extensive micropores for soft tissue engineering. ***Tissue Eng*** 12, 917-925 (2006).

150. Bain, J.R., Mackinnon, S.E. & Hunter, D.A. Functional evaluation of complete sciatic, peroneal, and posterior tibial nerve lesions in the rat. ***Plast. Reconstr. Surg.*** 83, 129-138 (1989).

151. de Medinaceli, L., Freed, W.J. & Wyatt, R.J. An index of the functional condition of rat sciatic nerve based on measurements made from walking tracks. ***Exp Neurol*** 77, 634-643 (1982).

152. de Medinaceli, L., Freed, W.J. & Wyatt, R.J. An index of the functional condition of rat sciatic nerve based on measurements made from walking tracks. ***Exp. Neurol.*** 77, 634-643 (1982).

153. Tactonic Farms, I. 2006).

154. Donadoni, C. et al. Improvement of combined FISH and immunofluorescence to trace the fate of somatic stem cells after transplantation. ***J. Histochem. Cytochem.*** 52, 1333-1339 (2004).